

GPS RTK-Based Attitude Determination for the e-POP Platform onboard the Canadian CASSIOPE Spacecraft in Low Earth Orbit

Don Kim and Richard B. Langley
Department of Geodesy and Geomatics Engineering, University of New Brunswick, Canada

BIOGRAPHY

Don Kim is a senior research associate in the Department of Geodesy and Geomatics Engineering at the University of New Brunswick (UNB). He has a bachelor's degree in urban engineering, and M.Sc.E. and Ph.D. degrees in geomatics, all from Seoul National University. Dr. Kim has been involved in GPS research since 1991 and active in the development of an ultrahigh-performance RTK system. He received the Dr. Samuel M. Burka Award for 2003 from The Institute of Navigation (ION).

Richard B. Langley is a professor in the Department of Geodesy and Geomatics Engineering at UNB, where he has been teaching and conducting research since 1981. He has a B.Sc. in applied physics from the University of Waterloo and a Ph.D. in experimental space science from York University, Toronto. Prof. Langley has been active in the development of GPS error models since the early 1980s and has been a contributing editor and columnist for GPS World magazine since its inception. He is a fellow of the ION and an associate fellow of the Royal Institute of Navigation. He shared the ION 2003 Burka Award with Don Kim.

INTRODUCTION

Over the last decade, GPS receivers have been successfully used for attitude and orbit determination on microsattellites and minisattellites in low Earth orbit [Purivigraipong et al., 1999; Purivigraipong and Unwin, 2001; Cross and Ziebart, 2002]. As a result, it has been a trend in space missions to use cost-effective GPS receivers for space science and engineering experiments. The use of commercial components for spacecraft GPS receivers has been experienced on some other space missions. However, it is so far restricted to low-grade single-frequency receivers and a limited range of correlator chipsets. The use of a fully commercial, geodetic grade dual-frequency receiver with no heritage in space applications has been recently considered for space missions [Langley et al., 2004; Montenbruck et al., 2006].

A rapid, precise and reliable GPS-based attitude determination system for satellites should be able to compete with existing space-deployed attitude systems such as star sensors. The precision of spacecraft GPS attitude determination is mostly at the 0.5-1.0 degree level [Campana et al., 1999; Giulicchi et al., 2000]. Unfortunately, due to the limited resources of microsattellites, most of the methods discussed in the papers would be difficult to run effectively in real time. In terms of attitude precision attainable from GPS attitude determination system, multipath and the baseline length between the antennas will be the principal limiting factors.

In this paper, we introduce our approach for a real-time GPS attitude determination system using commercial, geodetic grade dual-frequency GPS receiver, developed for the Enhanced Polar Outflow Probe (e-POP) platform onboard the Canadian CASSIOPE (the CAScade Smallsat and IOnospheric Polar Explorer) spacecraft to be flown in low Earth orbit.

SPACECRAFT DESIGN

CASSIOPE is a Canadian satellite scheduled for launch in 2008. It is a hybrid mission designed for a wide range of tasks including space-based communication and observations of the Earth's atmospheric environment. A dedicated suite of eight scientific instruments, called e-POP, will investigate space storms in the upper atmosphere and provide GPS-based navigation information. GAP (GPS Attitude and Profiling) is one of the eight scientific instruments. Figure 1 shows a concept view of the CASSIOPE spacecraft.

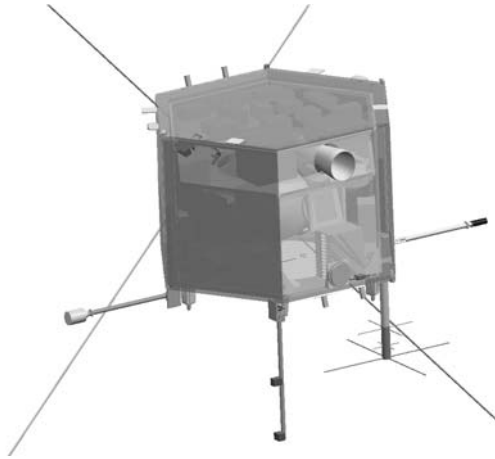


Figure 1. Conceptual view of the CASSIOPE spacecraft.

GAP Design

The design of GAP is based primarily on the use of commercial-off-the-shelf (COTS) GPS receiver technology. Early in the mission design, it was decided to base the GAP instrument on a COTS dual-frequency receiver rather than a space qualified one. The decision was based primarily on economics. NovAtel's OEM4-G2L dual-frequency receivers have been selected as the candidate hardware for this project. A series of tests were carried out to help determine the viability of using COTS GPS receivers for a satellite mission [Langley et al., 2004].

The GAP instrument has been designed and constructed in collaboration with Bristol Aerospace. Figure 2 shows the functional block diagram of the GAP instrument. The interface card used to interface the e-POP data handling unit with the receiver cards is based on Bristol Aerospace controller architecture with spaceflight heritage and an added FPGA (Field Programmable Gate Array). Some other components (such as patch antennas) also have spaceflight heritage.

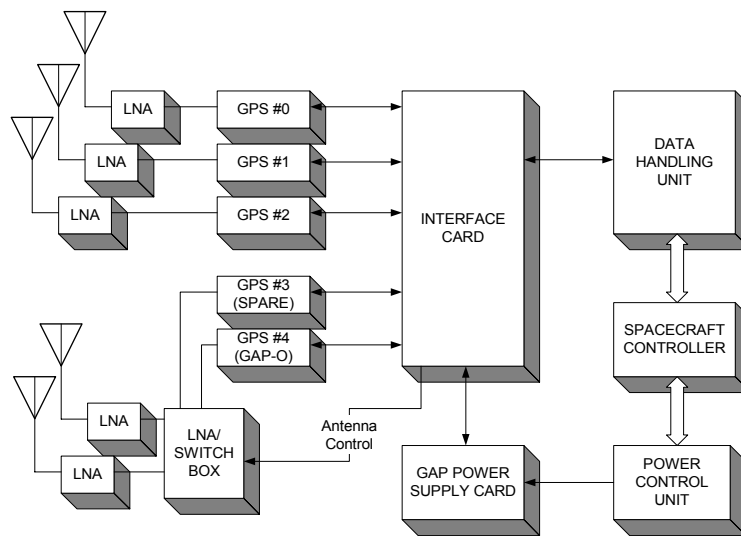


Figure 2. GAP instrument functional block diagram.

A total of five receivers on the satellite will be used for high precision navigation, attitude determination and radio occultation measurements. The four antennas to be used for navigation and attitude determination, together with their associated equipment called GAP-A, will be mounted on the zenith-facing side of the spacecraft and one antenna for occultation, together with its associated equipment called GAP-O, on the anti-ram (i.e., anti-velocity) side of the spacecraft. GAP-A collects and processes simultaneous observations from three of the GPS receivers. As illustrated in Figure 3, four receiving antennas including one spare will be mounted on the spacecraft. These antennas are mounted in locations to

minimize multipath reflections and maximize the baseline length between the antennas. GAP-O consists of a dual-frequency GPS receiver, with a switchable spare, to collect GPS occultation data at a 20 Hz data rate sufficient for ionospheric tomography science.

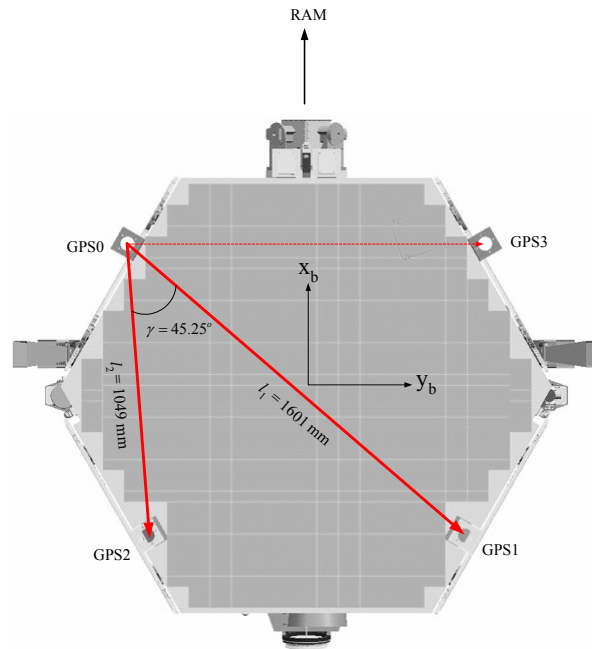


Figure 3. GAP-A antenna/baseline geometry.

GAP-A Performance Requirement

The GAP-A experiment will serve a number of purposes. It will provide an accurate absolute time reference, spacecraft position and velocity information to the data handling unit. Also, it will perform real-time spacecraft 3-axis attitude determination. The performance requirement of the GAP-A is summarized in Table 1. More precise results will be achievable by post-processing the down-linked data; e.g., 0.5 degree accuracy for post-processed attitude.

Table 1. GAP performance requirement.

Description	Accuracy (3σ)	Remark
Position	10 m	Real-time
Velocity	0.25 m/s	
Time	1 μ sec	
Attitude	5 deg	Real-time
	0.5 deg	Post-processed

RTK-BASED ATTITUDE DETERMINATION

The DD (double-differenced between satellites and receivers) carrier-phase observations are used for spacecraft attitude determination in our approach while the DD pseudorange observations are used for estimating nominal baseline components and float ambiguities. As illustrated in Figure 3, GPS0 is considered as the base station while GPS1 and GPS2 are considered as the rovers. GPS3 is the spare antenna. At each epoch, the navigation solution of GPS0 is taken as the Earth-centred Earth-fixed (ECEF) position of the spacecraft. The system is based on the general purpose UNB RTK (real-time kinematic) engine which has been used for various scientific and engineering applications [Kim and Langley, 2003; Kim et al., 2003]. It includes differential carrier-phase ambiguity resolution and position/velocity estimation. The attitude of the spacecraft is determined by estimating the rotation matrix between the body-fixed and ECEF frames using two baseline vectors (i.e., GPS1-GPS0 and GPS2-GPS0) and one vector orthogonal to them (i.e., the cross product of the two baseline vectors).

The Observation Model

The linearized DD carrier-phase observation model for single- and short-baseline (< 2 m) applications is given as:

$$\mathbf{y}_{i,j} = \mathbf{A}_j \mathbf{x}_j + \lambda_i \mathbf{N}_{i,j} + \mathbf{e}_{i,j}, \quad \text{Cov}[\mathbf{e}_{i,j}] = \mathbf{Q}_{\mathbf{y}_{i,j}} \quad (1)$$

and

$$\mathbf{A}_j = \begin{bmatrix} \frac{\partial \rho_j^1}{\partial x_j} & \frac{\partial \rho_j^0}{\partial x_j} & \frac{\partial \rho_j^1}{\partial y_j} & \frac{\partial \rho_j^0}{\partial y_j} & \frac{\partial \rho_j^1}{\partial z_j} & \frac{\partial \rho_j^0}{\partial z_j} \\ \vdots & & \vdots & & \vdots & \\ \frac{\partial \rho_j^m}{\partial x_j} & \frac{\partial \rho_j^0}{\partial x_j} & \frac{\partial \rho_j^m}{\partial y_j} & \frac{\partial \rho_j^0}{\partial y_j} & \frac{\partial \rho_j^m}{\partial z_j} & \frac{\partial \rho_j^0}{\partial z_j} \end{bmatrix} \text{ at } \mathbf{x}_{0j}, \quad (2)$$

where \mathbf{y} is the vector of DD carrier-phase observations in distance units; \mathbf{x} is the vector of unknown parameters including the baseline components (x , y and z); \mathbf{A} is the design matrix corresponding to \mathbf{x} ; \mathbf{x}_0 is the vector of nominal baseline components; ρ is the geometric range between a satellite and a rover; superscript m and subscript j indicate a satellite and a rover, respectively; superscript 0 indicates the reference satellite for the DD operation; \mathbf{N} is the vector of DD ambiguities; λ is the wavelength of the carrier-phase observations; \mathbf{e} is the noise vector including multipath and receiver system noise (here, the residual orbit error, and tropospheric and ionospheric delays are negligible); $\text{Cov}[\cdot]$ represents the variance-covariance operator; $\mathbf{Q}_{\mathbf{y}}$ is the variance-covariance matrix of the observations; and subscript i indicates the type of carrier-phase observations (e.g., L1, L2 or widelane).

For the real-time attitude system, the widelane carrier-phase observations are used in our approach. On the other hand, the L1 and L2 carrier-phase observations will be used for post-processed attitude determination to attain more precise attitude results. Normally, widelane ambiguity resolution is easier and more reliable compared with that for L1 and L2. More detailed reasoning for this approach is discussed in the ‘Validation’ section below.

The Baseline Constraint

When calculating spacecraft attitude, the baseline length between antennas (a pair consisting of the base and a rover) is assumed to be constant and known. By linearizing the expression for the baseline length, we can obtain a constraint on the unknown parameters as:

$$l_j = \mathbf{h}_j \mathbf{x}_j + \varepsilon_j, \quad \text{Var}[\varepsilon_j] = \sigma_{\varepsilon_j}^2, \quad (3)$$

and

$$\mathbf{h}_j = \begin{bmatrix} \frac{\partial l_j}{\partial x_j} & \frac{\partial l_j}{\partial y_j} & \frac{\partial l_j}{\partial z_j} \end{bmatrix} \text{ at } \mathbf{x}_{0j} \quad (4)$$

where l is the baseline length; \mathbf{x} is the vector of unknown parameters including the baseline components (x , y and z); \mathbf{h} is the design matrix corresponding to \mathbf{x} ; \mathbf{x}_0 is the vector of nominal baseline components; ε is the error in the known baseline length; $\text{Var}[\cdot]$ represents the variance operator; σ_{ε}^2 is the uncertainty of the baseline length; and again, subscript j indicates a rover (that is, a baseline associated with the rover).

Once the baseline length and its uncertainty are known, therefore, it is possible to treat the baseline constraint as an additional measurement available with a certain uncertainty at every epoch. Then, the augmented observation model is given by

$$\begin{bmatrix} \mathbf{y}_{i,j} \\ \vdots \\ l_j \end{bmatrix} = \begin{bmatrix} \mathbf{A}_j \\ \mathbf{h}_j \end{bmatrix} \mathbf{x}_j + \begin{bmatrix} \lambda_i \mathbf{I} \\ \mathbf{0} \end{bmatrix} \mathbf{N}_{i,j} + \begin{bmatrix} \mathbf{e}_{i,j} \\ \varepsilon_j \end{bmatrix}, \quad \text{Cov} \begin{bmatrix} \mathbf{e}_{i,j} \\ \varepsilon_j \end{bmatrix} = \begin{bmatrix} \mathbf{Q}_{y_{i,j}} \\ \vdots \\ \vdots \\ \sigma_{\varepsilon_j}^2 \end{bmatrix}, \quad (5)$$

where \mathbf{I} is an identity matrix; and $\mathbf{0}$ is a zero row vector. We use this augmented observation model in the subsequent ambiguity resolution.

Ambiguity Resolution

Least-squares estimation with integer constraint for the ambiguity parameters is referred to as an integer least-squares problem. The objective function to be minimized in the integer least-squares problem, Ω , is given as [Euler and Landau, 1992; Teunissen, 1995]:

$$\Omega_{i,j} = (\hat{\mathbf{N}}_{i,j} - \tilde{\mathbf{N}}_{i,j})^T \mathbf{Q}_{\hat{\mathbf{N}}_{i,j}}^{-1} (\hat{\mathbf{N}}_{i,j} - \tilde{\mathbf{N}}_{i,j}), \quad \text{with } \tilde{\mathbf{N}}_{i,j} \in \mathbb{Z}^m, \quad (6)$$

where $\hat{\mathbf{N}}$ is the vector of float ambiguity estimates; $\tilde{\mathbf{N}}$ is the vector of integer ambiguity candidates selected in the ambiguity search process; $\mathbf{Q}_{\hat{\mathbf{N}}}$ is the variance-covariance matrix of the float ambiguity estimates; \mathbb{Z} is the set of integers; m is the number of DD carrier-phase observations; and again, subscripts i and j indicate the type of carrier-phase observations and a rover, respectively.

Assuming that a search process for ambiguity parameters has been established, ambiguity candidates can be selected in the process. Then, we have to carry out the same procedure on each candidate sequentially until no ambiguity candidate remains. Then, our goal is to find the ambiguity candidate that minimizes the objective function in Eq. (6).

Validation

The UNB RTK engine resolves carrier-phase ambiguities using single epoch observations, which means instantaneous epoch-by-epoch ambiguity resolution. Due to the limited resources of the spacecraft, mainly power available for the real-time attitude system, its operation may take place only over a short time period (perhaps, for a few tens minutes or so). In this case, a filtering technique requiring a long convergence time for ambiguity resolution is not an appropriate approach. Instead, the carrier-phase ambiguities need to be resolved instantaneously at the current epoch.

Compared to the conventional filtering techniques such as a Kalman filter and a sequential least-squares estimator, the instantaneous epoch-by-epoch ambiguity resolution may not always provide reliable solutions. In fact, the ambiguity candidate that minimizes the objective function in Eq. (6) does not always guarantee correct ambiguities if using single epoch observations. To improve the reliability of ambiguity resolution in our approach, the following criteria for validation are used:

- Baseline lengths: $\|l_j\| = \|\mathbf{x}_j\|, \quad j = 1, 2, \quad (7)$

- Inner angle between two baseline vectors: $\gamma = \cos^{-1} \left(\frac{\mathbf{x}_1 \cdot \mathbf{x}_2}{\|\mathbf{x}_1\| \|\mathbf{x}_2\|} \right), \quad (8)$

where l and γ are known values. The ambiguities will be considered as correct ones if both criteria are satisfied with a certain uncertainty. In the real-time attitude determination system, the widelane carrier-phase observations are used for ambiguity resolution as previously mentioned. This is also to improve the reliability of ambiguity resolution.

Attitude Determination

The navigation frame (n-frame) is defined as a local geodetic frame which has its origin coinciding with that of the sensor frame, with the x-axis pointing towards geodetic north, z-axis orthogonal to the reference ellipsoid pointing down, and y-axis completing a right-handed orthogonal frame (i.e., the north-east-down system). On the other hand, the body frame (b-frame) is defined as an orthogonal axis set which is aligned with the roll, pitch and heading axes of a vehicle (i.e., forward-transversal-down system). A rotation matrix \mathbf{C}_b^n from b-frame to n-frame can be defined as:

$$\mathbf{C}_b^n = \begin{bmatrix} \cos \theta \cos \psi & -\cos \phi \sin \psi + \sin \phi \sin \theta \cos \psi & \sin \phi \sin \psi + \cos \phi \sin \theta \cos \psi \\ \cos \theta \sin \psi & \cos \phi \cos \psi + \sin \phi \sin \theta \sin \psi & -\sin \phi \cos \psi + \cos \phi \sin \theta \sin \psi \\ -\sin \theta & \sin \phi \cos \theta & \cos \phi \sin \theta \end{bmatrix}, \quad (9)$$

where ϕ , θ and ψ are the three Euler angles; i.e., roll, pitch and yaw, respectively. Then, the Euler angles can be determined from \mathbf{C}_b^n by the following equations:

$$\begin{aligned} \phi &= \text{atan2}(c_{32}, c_{33}) \\ \theta &= -\tan^{-1}\left(\frac{c_{31}}{\sqrt{1-c_{31}^2}}\right) \\ \psi &= \text{atan2}(c_{21}, c_{11}), \end{aligned} \quad (10)$$

where c_{ij} ($1 \leq i, j \leq 3$) is the (i,j) -th element of \mathbf{C}_b^n and atan2 is a four quadrant inverse tangent function. The coordinates of any one baseline in the b-frame and n-frame are related by

$$\mathbf{x}_{j,n} = \mathbf{C}_b^n \mathbf{x}_{j,b} \quad \text{or} \quad \mathbf{x}_{j,b} = (\mathbf{C}_b^n)^{-1} \mathbf{x}_{j,n} = \mathbf{C}_n^b \mathbf{x}_{j,n}, \quad j = 1, 2. \quad (11)$$

As illustrated in Figure 4, if the third baseline vector is defined as the vector orthogonal to the two baseline vectors \mathbf{x}_1 and \mathbf{x}_2 simultaneously; i.e.,

$$\mathbf{x}_{3,n} = \mathbf{x}_{1,n} \times \mathbf{x}_{2,n} \quad \text{and} \quad \mathbf{x}_{3,b} = \mathbf{x}_{1,b} \times \mathbf{x}_{2,b}, \quad (12)$$

then we have

$$\mathbf{X}_n = \mathbf{C}_b^n \mathbf{X}_b \quad \therefore \mathbf{C}_b^n = \mathbf{X}_n \mathbf{X}_b^{-1}, \quad (13)$$

where

$$\mathbf{X}_n = [\mathbf{x}_{1,n} \quad \mathbf{x}_{2,n} \quad \mathbf{x}_{3,n}] \quad \text{and} \quad \mathbf{X}_b = [\mathbf{x}_{1,b} \quad \mathbf{x}_{2,b} \quad \mathbf{x}_{3,b}]. \quad (14)$$

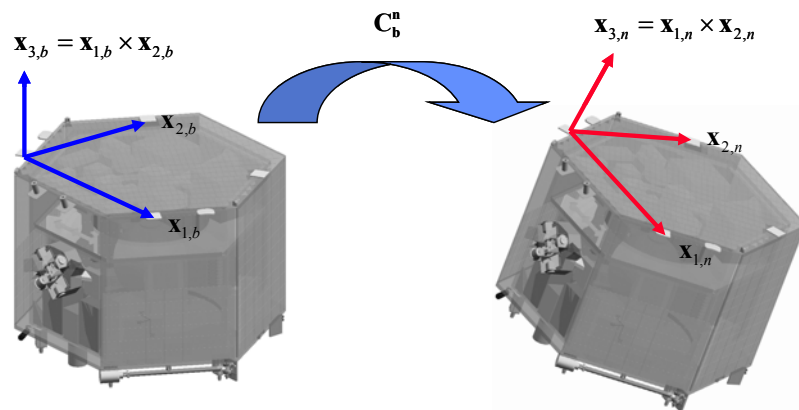


Figure 4. Attitude determination.

Unfortunately, the rotation matrix C_b^n obtained by Eq. (13) may not satisfy the orthogonality and normality condition. This problem can be resolved if we transform C_b^n into the Euler angles using Eq. (10), and then transform the Euler angles again into C_b^n using Eq. (9).

Issues on Initialization

To obtain the design matrices in Eqs. (2) and (4), \mathbf{A} and \mathbf{h} , the vector of nominal baseline components \mathbf{x}_0 should be determined. As the geometric range ρ is typically over 20,000 km, the design matrix \mathbf{A} is not sensitive to the errors in the nominal baseline components unless the errors are very large. On the other hand, the design matrix \mathbf{h} is very sensitive to the errors in the nominal baseline components due to the short-baseline condition (< 2 m). This can degrade the performance of ambiguity resolution in our approach. To improve its performance, therefore, we have to reduce the errors in the nominal baseline components. Three situations can be considered:

- Unstabilized mode: When the spacecraft is in maneuver, the pseudorange observations constitute the only information to determine the nominal baseline components. As the errors in the pseudorange observations can be as large as up to a few metres due to multipath and noise, the design matrix \mathbf{h} may not be correctly derived. This may result in wrong ambiguity resolution. To avoid this situation, the baseline constraint in Eq. (5) should be de-weighted.
- Stabilized mode: When the spacecraft is stabilized in space, the velocity estimates at GPS0 can be used to determine the nominal baseline components as illustrated in Figure 5. The nominal baseline components can be determined by the geometry of spacecraft velocity and baseline vectors.
- Full attitude mode: When spacecraft attitude information is available from previous epoch solution, the nominal baseline components can be directly determined using Eq. (11).

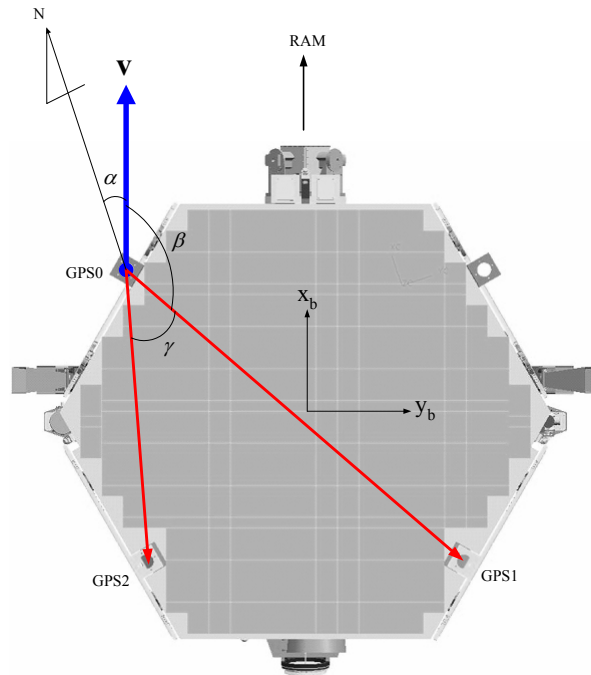


Figure 5. Spacecraft velocity and baseline vector geometry.

For ambiguity resolution, the float ambiguities and their variance-covariance matrix should be determined in Eq. (6). Considering the limited resources for the real-time attitude system, we have adopted a very simple approach to estimate them. The float ambiguities can be estimated using the pseudorange and carrier-phase observations at the current epoch as:

$$\tilde{\mathbf{N}}_{i,j} = \frac{1}{\lambda_i} (\mathbf{P}_i - \Phi_i), \quad (15)$$

where \mathbf{P} and Φ are the DD pseudorange and carrier-phase observations, respectively. Also, the variance-covariance matrix of the float ambiguity estimates can be derived by propagating the variance of the pseudorange and carrier-phase observations available from the receiver data log as:

$$\mathbf{Q}_{\hat{\mathbf{n}}_{i,j}} = \frac{1}{\lambda_i^2} (\mathbf{Q}_{\mathbf{p}_i} + \mathbf{Q}_{\Phi_i}) \quad (16)$$

where $\mathbf{Q}_{\mathbf{p}_i}$ and \mathbf{Q}_{Φ_i} are the variance-covariance matrices of the DD pseudorange and carrier-phase observations, respectively.

CONSIDERATIONS FOR 24-BIT PROCESSOR

The design of the GAP instrument interface is centered on Bristol Aerospace controller architecture with spaceflight heritage; e.g., the Motorola DSP56309 and the Actel A54SX72A FPGA. The digital signal processor (DSP) will work in conjunction with the FPGA to provide overall control of the instrument. The DSP will control the instrument data and address bus. The FPGA will act as the data interface between the DSP and most other internal and external devices.

As the Motorola DSP56309 is a 24-bit precision DSP, all ANSI C data types are supported, except double and long double, both of which are evaluated as floats [Motorola, 1999; Tasking, 2002]. Under this restriction, we were faced with one major problem in developing the real-time attitude determination software. To obtain navigation and attitude solutions, raw GPS data should be read. Unfortunately, many GPS-related parameters and observations need to be represented in double-precision. Therefore, we had to write software to convert double-precision variables into single-precision ones. To accomplish the goal, we used the following approaches:

- Avoid direct use of double-precision variables in floating point operation. If data logs associated with the satellite and receiver positions are available from the receiver output, we can avoid double-precision computation relevant to the satellite and receiver positions since these are of sufficient precision for our needs.
- Perform bit-wise operation on the double-precision carrier-phase observations to separate them into the integer and fraction parts (Figure 6). Then, execute double-differencing between satellites and receivers for the integer part as well as the fraction part. Later, combine the double-differenced integer and fraction parts. This manipulation will result in small single-precision values.

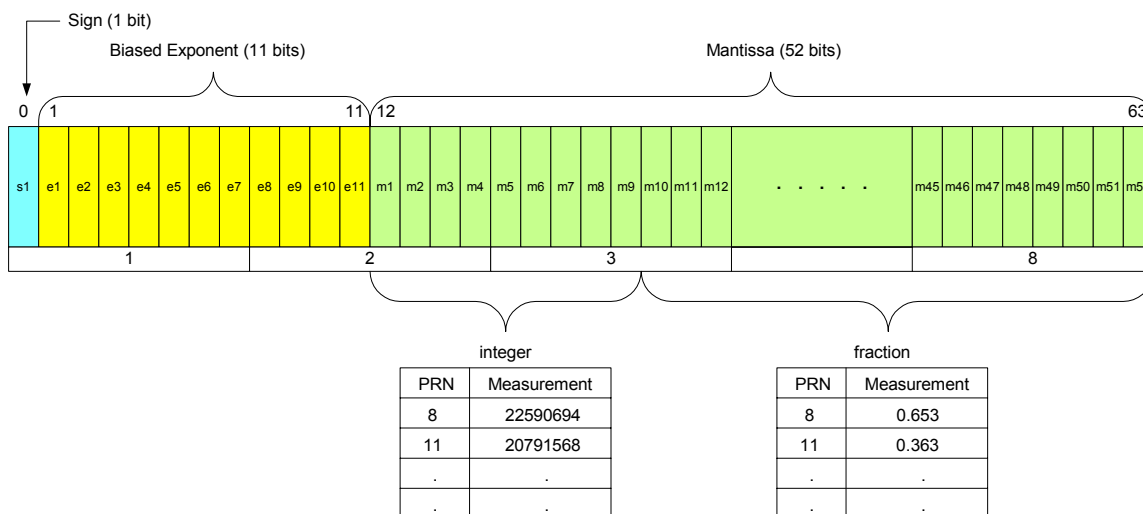


Figure 6. Double-precision floating point format.

The NovAtel OEM4 receiver group is capable of generating many different types of data logs [NovAtel, 2003]. For RTK processing, we normally use two data logs, RANGECMP (Message ID: 140) and RAWEPHEM (Message ID: 41). RANGECMP is the compressed version of the RANGE log (Message ID: 43) that contains the channel measurements for

the currently tracked satellites. The RAWEPHEM log is the raw ephemeris log that contains the raw binary information for subframes one, two and three of the satellite navigation message with the parity information removed. Using these data logs, we can compute satellite and receiver positions at a given epoch. Unfortunately, the computation involves double-precision floating point operations. To avoid direct use of double-precision floating point operations, we use the SATXYZ log (Message ID: 270) for satellite position in ECEF Cartesian coordinates. Also we use the PSRXYZ (Message ID: 243) and PSRPOS (Message ID: 47) logs for receiver position in ECEF Cartesian and local geodetic coordinates, respectively.

PERFORMANCE TEST

To demonstrate the capabilities of the attitude software, three different hardware systems were used as GAP software test beds, including a laptop computer, the Bristol SPP (System Platform Processor) controller, and the GAP interface card EM (Express Module). The Bristol SPP controller is a multipurpose controller board developed for sounding rocket missions. It features a Motorola DSP56309, 128 KB SRAM (Static Random Access Memory) memory, Flash Memory, and two RS-232 serial ports. The GAP interface card EM is based on the Bristol STARS controller architecture with added FPGA.

As illustrated in Figure 7, a 3-axis motion table was built using stepper motors and stepper motor controllers (Pontech STP100). Also, an Ethernet-to-serial controller (Sollae EZL-400s) was integrated in the test bed. This add-on device enabled the motion table to be accessed and controlled from a remote place. The rotation angles measured by each stepper motor can be used as the reference of attitude solutions computed using the three GPS receivers. To accomplish this end, the stepper motors and GPS receivers should be synchronized in time. This has not been completed yet.

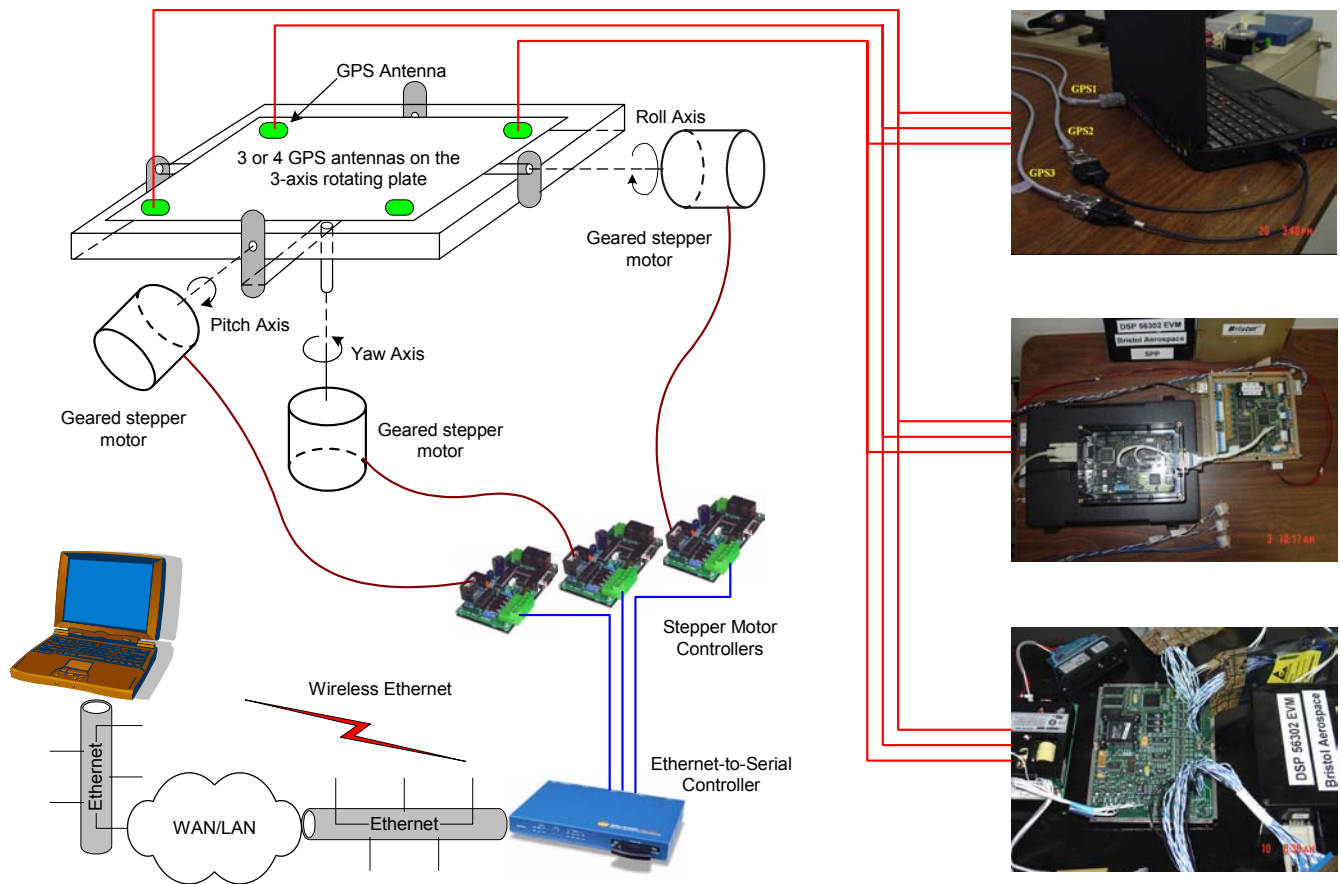


Figure 7. GAP software test bed configuration.

To test the attitude software while communicating with up to three GPS receivers, a real-time attitude determination test was performed on a laptop computer (Pentium 4-M 1.8 GHz IBM T30). The experiment configuration is illustrated in Figure 8. The test was performed on the roof of Gillin Hall on the University of New Brunswick Fredericton campus. Due to the penthouse of Gillin Hall and buildings in the vicinity of the GPS antennas, we could test the attitude software in a

multipath-rich environment. This situation was useful in analyzing its performance under the worst case scenario of GPS attitude determination.

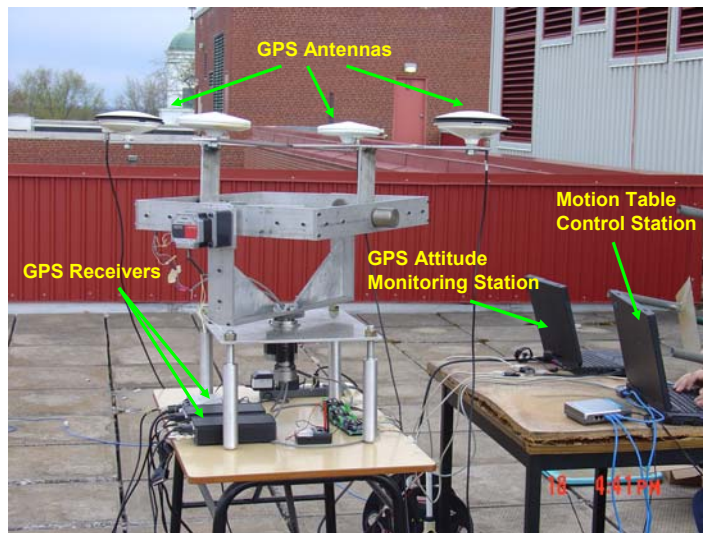


Figure 8. Real-time attitude determination experiment configuration.

Figure 9 illustrates the output of the attitude software on the laptop computer. During the test, the motion table was in a static mode. This situation made it easy to evaluate overall performance of the attitude software. At each epoch, two baseline vectors were computed by the UNB RTK engine as shown in the left panel. To obtain the baseline solutions, the widelane observations were processed and their ambiguities were fixed. The right panel in Figure 9 shows that all of the attitude solutions were determined within 5-degree accuracy. This result satisfies excessively the real-time attitude requirement in Table 1.

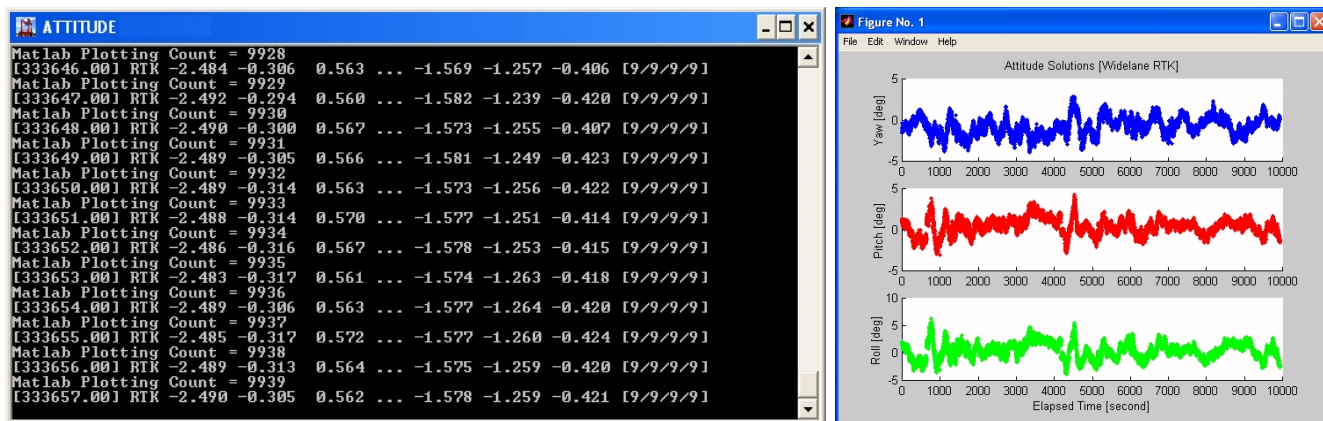


Figure 9. Real-time attitude determination test on a laptop computer: RTK solutions for two static baselines (left) and Matlab plot of attitude solutions, interfaced with the Microsoft Visual C++ 6.0 compiler (right).

The motion of a spacecraft was simulated by generating rotations on the yaw, pitch and roll axes. As shown in Figure 10, two baseline vectors were computed epoch-by-epoch after fixing the ambiguities of widelane carrier-phase observations. Compared with the horizontal solutions (i.e., northing and easting) in Figure 10, the vertical solutions (i.e., up) seem to be noisier. Fundamentally, this is due to a poor GPS geometry in the vertical direction. As a result, the pitch and roll solutions seem to be noisier than the yaw solutions in Figure 11. Unfortunately, we could not compare the attitude solutions with the rotation angles measured by each stepper motor because the stepper motors and GPS receivers were not synchronized in this test. By triggering the stepper motors with a GPS time-stamped command on receiving GPS data logs, we could synchronize both angle and attitude solutions to within microsecond-level latency. We plan to complete this task in the near future.

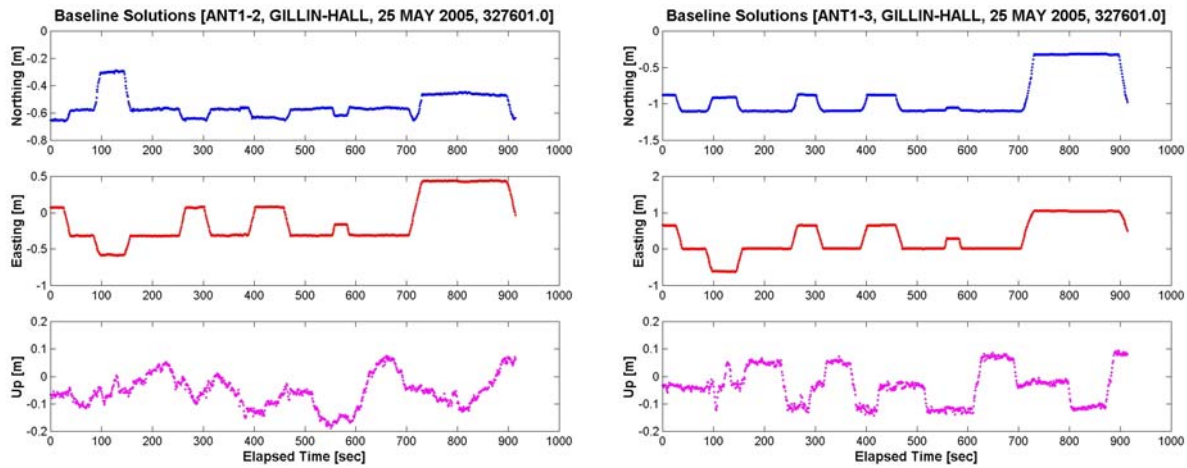


Figure 10. RTK solutions for two baselines in a kinematic mode.

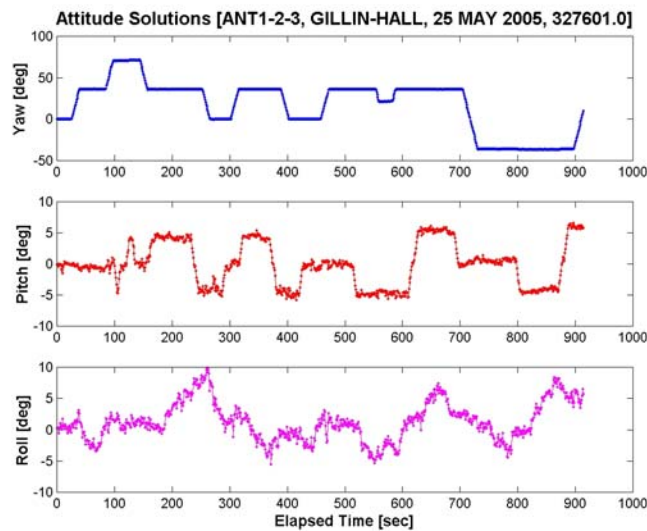


Figure 11. Attitude solutions corresponding to the RTK solutions for two baselines.

Subsequently, the PC-version attitude software was integrated into the software for the Bristol STARS controller developed with Tasking's C compiler (version 3.5). Actually, the Bristol STARS controller software provided the platform for developing the attitude software prior to installation on the GAP board. To communicate with the Bristol SPP controller and the GAP interface card EM via the Bristol DSP56309 EVM (EVALUATION MODULE), the Tasking CrossView debugger was used.

The DSP used for both the SPP and the EM has two data memory areas: X and Y. The base memory inside the processor has the same 4 KB for each X and Y memory area. There is an external 128 KB SRAM chip on the SPP that is mapped to Y memory. The EM has an external 256 KB SRAM for Y memory. By default, the Tasking's C compiler allocates data in X memory unless specified otherwise. So, the variables and data defined by the attitude software should be located in Y memory. Otherwise, the attitude software will be running out of memory. The final version of attitude software is designed to fit in 256 KB memory.

CONCLUDING REMARKS

Out of a dedicated suite of eight scientific instruments for the e-POP mission, GAP provides an accurate absolute time reference, spacecraft position and velocity information to the data handling unit. Also, it will perform spacecraft 3-axis attitude determination. Due to the limited resources of the spacecraft available for GAP real-time attitude determination, its operation may take place only over a short time period. For that reason, our approach to resolve carrier-phase ambiguities is

based on epoch-by-epoch ambiguity resolution, which resolves ambiguities instantaneously at the current epoch. At each epoch, two baseline vectors are computed by the UNB RTK engine, and then they are converted into the attitude solutions. To satisfy the real-time attitude requirement of 5-degree accuracy at the 3-sigma level, the widelane carrier-phase observations are used in our approach. The tests conducted so far provide good evidence for a proper functioning of the attitude software.

Further testing of GAP will be carried out at the University of Calgary's Institute for Space Research, which is leading the development of e-POP, and at Bristol Aerospace. Subsequently, additional testing will take place during the spacecraft assembly, integration and test program for the e-POP payload at the Canadian Space Agency's David Florida Laboratory in Ottawa.

ACKNOWLEDGEMENTS

The hardware system (the Bristol SPP controller and the GAP interface card EM) discussed in the paper has been lent by Bristol Aerospace for testing GAP software. The authors would like to thank Alexis Denis at Bristol Aerospace for his kind support and many useful discussions and the e-POP team at the University of Calgary's Institute for Space Research for their advice and help in managing the development, construction and testing of GAP. The authors would also like to thank Luis Serrano in the Department of Geodesy and Geomatics Engineering at UNB (currently working at Leica Geosystems AG, Heerbrugg, Switzerland) for performing experiments using the 3-axis motion table. Special thanks to NovAtel and Sollae Systems for providing equipment necessary to conduct this research. The GAP development work and associated space science research at UNB is supported by the Canadian Space Agency and the Natural Sciences and Engineering Research Council of Canada.

REFERENCES

- Campana, R., L. Marradi and S. Bonfanti (1999). "GPS attitude determination by adaptive Kalman filtering." Proceedings of ION GPS 1999, 12th International Technical Meeting of the Satellite Division of The Institute of Navigation, Nashville, TN, 14-17 September, pp. 1979-1988.
- Cross, P. and M. Ziebart (2002). "LEO GPS attitude determination algorithm designed for real-time on-board execution." Proceedings of ION GPS 2002, 15th International Technical Meeting of the Satellite Division of The Institute of Navigation, Portland, OR, 24-27 September, pp. 1051-1063.
- Euler, H.-J. and H. Landau (1992). "Fast GPS ambiguity resolution on-the-fly for real-time application." Proceedings of Sixth International Geodetic Symposium on Satellite Positioning, Columbus, Ohio, 17-20 March, pp. 650-659.
- Giulicchi, L., L. Boccia, G. Di Massa and G. Amendola (2000). "Performance improvement for GPS-based attitude determination systems." Proceedings of ION GPS 2000, 13th International Technical Meeting of the Satellite Division of The Institute of Navigation, Salt Lake City, UT, 19-22 September, pp. 2209-2215.
- Kim, D. and R. B. Langley (2003). "On ultrahigh-precision positioning and navigation." *Navigation: Journal of The Institute of Navigation*, Vol. 50, No. 2, Summer, pp. 103-116.
- Kim, D., R. B. Langley, J. Bond and A. Chrzanowski (2003). "Local deformation monitoring using GPS in an open pit mine: Initial study." *GPS Solutions*, Vol. 7, No. 3, December, pp. 176-185.
- Langley, R. B., O. Montenbruck, M. Markgraf and D. Kim (2004). "Qualification of a commercial dual-frequency GPS receiver for the e-POP platform onboard the Canadian CASSIPOE spacecraft." Proceedings of NAVITEC '2004, the 2nd ESA Workshop on Satellite Navigation User Equipment Technologies, ESTEC, Noordwijk, The Netherlands, 8-10 December 2004, pp. 397-405.
- Montenbruck O., M. Garcia-Fernandez and J. Williams (2006). "Performance comparison of semicodeless GPS receivers for LEO satellites." *GPS Solutions*, Vol. 10, No. 4, November, pp. 249-261.
- Motorola (1999). DSP56309EVM user's manual, DSP56309EVMUM/D, Rev. 1.92, 12/1999, Board Rev. 1.2, Motorola Inc., Austin, TX.
- NovAtel (2003). OEM4 Family of Receivers User Manual - Vol. 2 Command and Log Reference, OM-20000047, Rev. 12, 2003/07/31, NovAtel Inc., Alberta, Canada.
- Purivigraipong, S., Y. Hashida and M. J. Unwin (1999). "GPS attitude determination for microsattellites." Proceedings of ION GPS 1999, 12th International Technical Meeting of the Satellite Division of The Institute of Navigation, Nashville, TN, 14-17 September, pp. 2017-2026.
- Purivigraipong, S. and M. J. Unwin (2001). "Determining the attitude of a minisatellite by GPS." *GPS World*, Vol. 12, No. 6, June, pp. 60-66.
- Tasking (2002). DSP56xxx v3.5 C++ compiler user's guide, MA039-012-00-00, Doc. Ver. 1.53, Altium Ltd., Carlsbad, CA.

Teunissen, P. J. G. (1995). "The least-squares ambiguity decorrelation adjustment: A method for fast GPS integer ambiguity estimation." *Journal of Geodesy*, Vol. 70, No. 1-2, November, pp. 65-82.